Evolution of the colour-magnitude relation of early-type galaxies in cosmological numerical simulations

L.J. Zenocratti[1,2], A.V. Smith Castelli[1,2], M.E. De Rossi[3,4] & F.R. Faifer[1,2]

[1] *Facultad de Ciencias Astronómicas y Geofísicas, UNLP, Argentina*
[2] *Instituto de Astrofísica de La Plata, CONICET–UNLP, Argentina*
[3] *Ciclo Básico Común, UBA, Argentina*
[4] *Instituto de Astronomía y Física del Espacio, CONICET–UBA, Argentina*

Contact / lzenocratti@fcaglp.unlp.edu.ar

Resumen / En este trabajo estudiamos la evolución con el corrimiento al rojo de la relación color-magnitud (CMR, por sus siglas en inglés) de galaxias de tipo temprano. Esta evolución es analizada a partir de simulaciones numéricas cosmológicas, desde $z = 2$ hasta $z = 0$. Los resultados preliminares mostrados aquí representan el punto de partida de un estudio apuntado a identificar los procesos que originaron la CMR de galaxias de tipo temprano observada a $z = 0$.

Abstract / In this work, we study the evolution with redshift of the colour-magnitude relation (CMR) of early-type galaxies. This evolution is analyzed through cosmological numerical simulations from $z = 2$ to $z = 0$. The preliminary results shown here represent the starting point of a study aimed at identifying the processes that originated the observed CMR of early-type galaxies at z = 0.

Keywords / galaxies: evolution — galaxies: elliptical and lenticular, cD — cosmology: theory

1. Introduction

In the colour-magnitude diagram (CMD), early-type (ET) galaxies trace a well-defined sequence from dwarfs to giants, where brighter galaxies tend to be redder (e.g., Chen et al., 2010; Smith Castelli et al., 2013; Roediger et al., 2017). This colour-magnitude relation (CMR) is considered as universal, in the sense that it is observed with similar slopes in rich groups and clusters in the local Universe ($z \sim 0$). This sequence is interpreted as a mass-metallicity relation, with brighter and redder galaxies tending to be more massive and more metal-enriched (Sánchez-Blázquez et al., 2006; Conroy et al., 2014). Nevertheless, processes that establish and define it are not yet totally known for certain (e.g., Roediger et al., 2011; Janz et al., 2017; Connor et al., 2019).

In this work, we present a preliminary study that extends a previous analysis of the CMD for ET galaxies extracted from cosmological numerical simulations, studying the behaviour of the diagram as function of redshift. Our main goal is to provide clues that explain the origin of the CMR through the study of its evolution since the formation times of these galaxies until today.

2. Simulated galaxies

2.1. The EAGLE simulations

In this work, we use simulations of the Evolution and Assembly of GaLaxies and their Environments (EAGLE) project (Schaye et al., 2015; McAlpine et al., 2016), a suite of cosmological, hydrodynamical simulations of a standard ΛCDM universe, that were performed by using a modified version of the GADGET-3 code (Springel, 2005; Schaller et al., 2015). The cosmological parameters used for the EAGLE simulations are those of the Planck Collaboration (Planck Collaboration et al., 2014): $\Omega_\Lambda = 0.693$, $\Omega_m = 0.307$, $\Omega_b = 0.048$ and $h = 0.6777$. We started working with the reference, intermediate-resolution simulation Ref-L0100N1504, which has a box size of 100 co-moving Mpc, with an initial baryonic particle mass of 1.81×10^6 $M_\odot$ and a maximum proper softening length of 0.70 proper kpc.

The identification of galaxies in the simulations were carried out by applying a Friends-of-Friends technique (Davis et al., 1985), combined with the SUBFIND algorithm (Springel et al., 2001; Dolag et al., 2009). The subgrid physics in EAGLE simulations implement prescriptions for radiative cooling and heating, star formation, chemical enrichment, supernovae and active galactic nuclei feedbacks, and interactions and fusions, among other processes (see Schaye et al., 2015 for details).

2.2. Galaxy selection

From the Ref-L0100N1504 EAGLE simulation, we extracted galaxies with stellar mass $M_\star \geqslant 10^9$ $M_\odot$, a star formation rate (SFR) such that $\log(SFR/M_\star) \leqslant -11$ yr^{-1}, and a star forming gas fraction $M_{SF\ gas}/(M_{SF\ gas} + M_\star) \leqslant 0.1$ (Zenocratti et al., 2018). Galaxies fulfilling these conditions are defined as our simulated sample of ET galaxies. At all analysed redshifts, our sample of selected galaxies is constituted by more than 9 500 systems with stellar

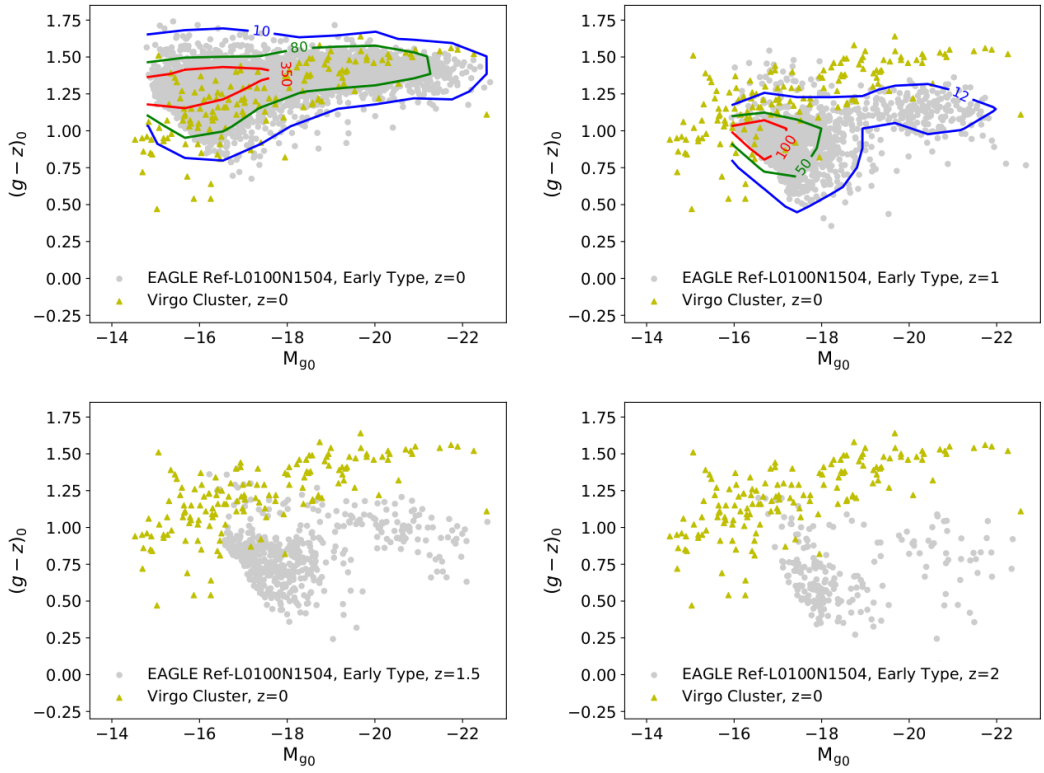

Figure 1: Colour-magnitude diagrams of early-type galaxies at different redshift z. Grey circles are simulated galaxies, extracted from the EAGLE Ref-L0100N1504 simulation using the selection criteria stated in Section 2.2.. Yellow triangles are galaxies of the Virgo Cluster (Chen et al., 2010; Sánchez-Janssen et al., 2019). Different panels show the CMD at $z = 0$ (top left), $z = 1$ (top right), $z = 1.5$ (bottom left), and $z = 2$ (bottom right). Three contours of constant number of galaxies are shown for $z = 0$ and $z = 1$.

masses higher than 10^9 $M_\odot$. To check our selection criteria, we compared the CMD of that sample at $z = 0$ with the corresponding to ET galaxies in the Virgo Cluster (Chen et al., 2010; Sánchez-Janssen et al., 2019). The CMD of the simulated sample at $z = 0$ agrees with the observed one (see Fig. 1).

3. Results

3.1. CMR at different z

Panels of Fig. 1 show the simulated $(g - z)_0$ vs. M_{g0} CMD from $z = 0$ to $z = 2$ (grey circles); for comparison, galaxies of the Virgo Cluster ($z \approx 0$) are shown in every panel (yellow triangles). As can be seen, the simulated sample and the observed one at $z = 0$ are located in the same region of this CMD, therefore our selection criteria lead to a sample of simulated galaxies which follows the observed trends. Also, some contours of constant number of simulated galaxies are plotted in the first two panels (i.e., at $z = 0$ and $z = 1$), in order to identify which region of the $(g - z)_0$ vs. M_{g0} plane is more densely populated. As can be seen, when z decreases the number of ET galaxies increases in both luminosity extremes. That increment seems to be higher in the less luminous region of the CMD. Also, at lower z the bulk of galaxies in the CMD is located in redder regions. Finally, it can be seen that the brightest region of the CMD is always populated.

3.2. Distributions of magnitudes and colours at different z

The panels of Fig. 2 show the distributions of magnitude M_{g0} and colour $(g-z)_0$ for redshifts from $z = 0$ to $z = 2$, for the simulated sample of ET galaxies. With respect to the distribution in magnitude, the low-magnitude peak moves towards less luminous magnitudes at lower z. Also, at $z = 2$ a bimodality can be seen, with a peak at $M_{g0} \approx -18$ and another (much less prominent) peak at $M_{g0} \approx -21$. As z decreases, the brightest peak vanishes and the faintest galaxies become the dominant population, which is in agreement with observations: at z=0 faint ET galaxies are much more abundant than bright ET galaxies. In addition, as z decreases, the faint peak of the luminosity distribution moves towards faintest magnitudes showing that the faintest end of the CMR is the last region to be populated in the CMD, within our considered mass range ($M_\star > 10^9$ $M_\odot$).

The distribution of colour $(g - z)_0$ shows that at lower z, the peak of the distribution moves towards redder colours, being this distribution narrower, i.e., the scatter in colour seems to decrease towards lower z. This means that simulated ET galaxies (selected with our criteria) tend to be bluer in the past, showing colours

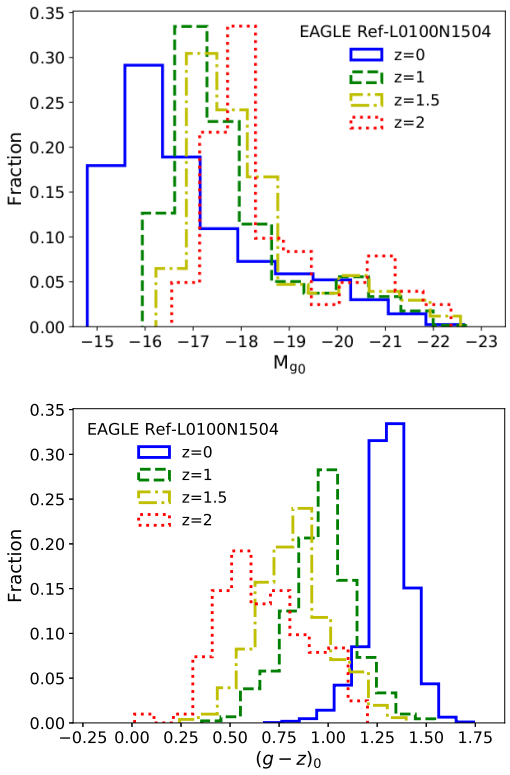

Figure 2: Distribution of M_{g0} magnitude (top) and $(g-z)_0$ colour (bottom) at different redshift z for the simulated sample of ET galaxies, extracted from the EAGLE Ref-L0100N1504 simulation. The histograms correspond to $z = 0$ (blue solid), $z = 1$ (green dashed), $z = 1.5$ (yellow dot-dashed), and $z = 2$ (red dotted).

within a little broader range than observed today. In particular, the bluest galaxies at high redshift might be ET galaxies going through their final stages of star formation. The shift of the maximum with z towards redder colours might be due to an increase in the average age, while the lower scatter towards $z = 0$ might indicate that $(g-z)_0$ is not sensitive to age variations within the population. Specific properties of our simulated sample (such as masses, ages, SFRs, metallicities, among others) will be studied exhaustively in a forthcoming work.

4. Conclusions and further work

We started studying the evolution with redshift of the CMR for simulated ET galaxies, extracted from the EAGLE Ref-L0100N1504 simulation. Our selected sample of simulated $z = 0$ galaxies is consistent with the observed CMD for ET galaxies in the Virgo Cluster. Therefore, we also used these criteria to select ET galaxies up to $z = 2$. In the CMD, ET galaxies are placed in bluer regions with increasing z. At lower z, the number of systems with lower luminosities increases, and ET galaxies tend to be redder, with a decreasing scatter in the colour distribution. Blue and bright ET galaxies present at higher z might be systems still in development.

In a future work, additional properties of the selected sample of ET galaxies (mass, metallicities, SFRs, etc.) will be studied in detail. The evolution of such properties will be analysed comprehensively, as well as the evolution of dynamics and kinematics in these systems, aiming at better understand the setting of the CMR up until the present. Also, other EAGLE simulations with variations in the subgrid physics will be used, in order to determine how variations in parameters affect the CMR.

Acknowledgements: We acknowledge Asociación Argentina de Astronomía for giving us the space to show our results. We acknowledge support from PICT-2015-3125 of ANPCyT, PIP 112-201501-00447 of CONICET and G151 of UNLP (Argentina). We acknowledge the Virgo Consortium for making their simulation data available. The EAGLE simulations were performed using the DiRAC-2 facility at Durham, managed by the ICC, and the PRACE facility Curie based in France at TGCC, CEA, Bruyèresle-Châtel.

References

Chen C.W., et al., 2010, ApJS, 191, 1
Connor T., et al., 2019, ApJ, 875, 16
Conroy C., Graves G.J., van Dokkum P.G., 2014, ApJ, 780, 33
Davis M., et al., 1985, ApJ, 292, 371
Dolag K., et al., 2009, MNRAS, 399, 497
Janz J., et al., 2017, MNRAS, 468, 2850
McAlpine S., et al., 2016, Astron. Comput., 15, 72
Planck Collaboration, et al., 2014, A&A, 571, A16
Roediger J.C., et al., 2011, MNRAS, 416, 1996
Roediger J.C., et al., 2017, ApJ, 836, 120
Sánchez-Blázquez P., et al., 2006, A&A, 457, 787
Sánchez-Janssen R., et al., 2019, ApJ, 878, 18
Schaller M., et al., 2015, MNRAS, 454, 2277
Schaye J., et al., 2015, MNRAS, 446, 521
Smith Castelli A.V., et al., 2013, ApJ, 772, 68
Springel V., 2005, MNRAS, 364, 1105
Springel V., Yoshida N., White S.D.M., 2001, NewA, 6, 79
Zenocratti L.J., et al., 2018, BAAA, 60, 127